1838

Emergence of structural anisotropy in Optical Glasses treated to support Second Harmonic Generation

C. Cabrillo
Instituto de Optica, Serrano 121, 28006, Madrid, Spain. Tel: 34-91-5616800, Fax: 34-91-5855184, email: ccabrilo@foton0.iem.csic.es

P. García-Fernández, F.J. Bermejo
Instituto de Estructura de la Materia, Serrano 123, 28006, Madrid, Spain. Tel: 34-91-5616800, Fax: 34-91-5855184, P.G.'s email: empris@iem.csic.es, F.J.B.'s email: embermejo@iem.csic.es

V. Pruneri, P. G. Kazansky
Optoelectronics Research Centre, University of Southampton,
Southampton S017 IBJ, United Kingdom. Tel: 44-1703-593083, Fax: 44-1703-593149, V.P.'s email: VP3@orc.soton.ac.uk

Few discoveries have puzzled the optics community more than the emergence of visible (green) light from optical fibers after strong irradiation by an infrared laser [1]. This frequency-doubling phenomenon known as Second Harmonic Generation (SHG) is not expected to take place in a centrosymmetric material such as the amorphous silica fiber-core, which shows no measurable second-order optical susceptibility $\chi^{(2)}$ [2]. The process to be efficient also requires well defined phase-matching between the interacting waves to allow for constructive interference, and this seems even more difficult to fulfill within the glassy medium. Several plausible explanations about the origin of the phenomenon have been put forward. One of the most widely accepted [3] does not involve structural modifications to accomplish the breakdown of the glass radial symmetry. Rather, it postulates the emergence of a spatially modulated local dc field, E_0, which, via a third-order nonlinearity ($\chi^{(3)}$) (finite in isotropic materials), induces a spatially modulated second order nonlinearity ($\chi^{(2)} \propto \chi^{(3)} E_0$) able to double the pump frequency. The achievement of a permanent $\chi^{(2)}$ in optical glasses has focused a large research effort, which lead to the discovery of alternative poling techniques. In actual fact, the phenomenon can be produced by application of a high voltage (~ 5 kV, just below dielectric breakdown) to glass plates at moderate temperatures ($\sim 540 - 580$ K, compared with ≈ 1475 K where the glass melts). This method, known as "thermal" poling [4], provides permanent second-order nonlinear responses comparable to those shown by inorganic crystals. Whether the mechanism(s) leading to the emergence of a second order nonlinearity in "thermally-poled" glasses differ from those of photoinduced SHG or not needs to be clarified. At any rate, the relevant point stems from the possibility this method has opened up for developing inexpensive integrated optical frequency converters and electro-optic modulators.

We have performed a series of neutron scattering experiments to investigate the microscopic mechanisms leading to the appearance of SHG in "thermally" poled glasses [5,6]. In this summary we review the microscopic structure alterations we have found using diffraction means. Concomitant perturbations of the microscopic dynamics have been also detected by means of inelastic neutron scattering (See [5,6]).

The samples were made of electrically-fused quartz (Infrasil, Heraeus) with dimensions $40 \times 40 \times 0.1$ mm^3. The thickness (~ 100 μm) was chosen as the smallest possible, in order to increase the poled/unpoled volume ratio. In fact, after treatment [4], the nonlinearity is confined to a region ~ 5 μm deep under the anode surface regardless of the sample thickness. Poling was carried out at 548 K under an applied dc voltage of ~ 5 kV for 40 minutes. The poled sample consisted in fifteen plates stacked together. For comparison a similar stack of native samples was used. The measurements were performed using the LAD, time-of-flight diffractometer and the MARI spectrometer, both at the ISIS pulsed neutron source (R.A.L., UK). Those carried out at the diffractometer sought to detect indications of local anisotropy induced by poling. To see this, sets of two runs with the samples oriented ±45° with respect to the incident beam, were performed. The diffractometer consists in an array of 14 neutron counters covering a 2π angular range at discrete intervals each one spanning a large extent of momentum-transfers. In particular, our interest will here be focused on the analysis of those detectors ±90° with respect to the incident beam which span momentum-transfers covering directions mostly normal and parallel to the plates. Two spectra for both directions of momentum-transfers are then obtained with the corresponding detectors interchanged. In doing so, exploration along the direction of the field ap-

submitted to BPGG 99 - 'Bragg gratings, Photosensitivity, and Poling in Glass Waveguides'
Stuart, Florida, 23-25 Sept. 99

plied during poling and normal to it is envisaged. After averaging over both orientations, systematic errors are minimized.

The experimentally-accessible quantity of interest is here the static pair correlation function $d_{\|,\perp}(r)$ or alternatively, the radial distribution function $g_{\|,\perp}(r)$, both related to the observable static structure factor $S(Q)$ by a sine-Fourier transform, $d_{\|,\perp}(r) = 4\pi\rho r[g_{\|,\perp}(r) - 1] = \frac{2\pi}{Q}\int dQQ(S_{\|,\perp}(Q) - 1)\sin(Qr)$. The subscripts refer to directions parallel or normal to the stack of plates and ρ stands for the average number-density of the glass. The $d_{\|,\perp}(r)$ contains information about the thermally-averaged distribution of interatomic distances. For low values of r one expects to find sharp peaks corresponding to distances separating directly bonded atoms, such as Si–O or those O–O, which result from a pair of atoms linked to a common Si nucleus. At larger distances the structure is progressively washed out because of the static disorder and no measurable hints of ordering are expected well beyond some 20 Å.

The Fig. 1 depicts the $g_{\|,\perp}(r)$ functions measured for the poled plates and compared to that obtained for the native glass. A glance to the curves drawn there reveals a large difference in static correlations of the poled samples between parallel and perpendicular directions concerning distances within the 2.8 – 3.4 Å range. The graphs of the native samples serve to quantify any source of systematic error. The shortest distance, which corresponds to Si–O bonds, appears at 1.6175 (6) Å and that regarding O–O correlations shows up at 2.641 (1) Å. The differences between measurements mostly parallel and normal to the native glass plates are very small (differences in peak position of 2×10^{-3} Å and 7×10^{-3} Å in width). In contrast, the curves for the poled samples show that: (a) $g_{\|}(r)$ is basically unchanged after poling, (differences in the peak center and linewidth are, within the error bars indistinguishable from those of the unpoled plates), (b) $g_{\perp}(r)$ of the poled glass shows a peak at distances characteristic of Si–Si correlations significantly wider than that of the native sample, and (c) clear hints of a bimodal distribution of Si–Si distances are seen in the latter function. In other words, the difference between $g_{\|}(r)$ and $g_{\perp}(r)$ unequivocally shows the presence of an exceedingly strong anisotropy at scales of about 3 Å, which correspond to Si–Si correlations, that is, to distances between the centers of neighboring tetrahedra. More specifically, after a decomposition of the $g_{\|,\perp}(r)$ functions below 5 Å into a sum of Gaussians, the Si–Si peak appears in the native sample centered at 3.060 (9) Å with a width of 0.115 (8) Å in both $\|$ and $\perp$ directions. The peak shape of the same feature in $g_{\perp}(r)$ for the poled plates can be reproduced by addition of a further Gaussian which is now centered at 3.228 (23) Å and has a width of 0.106 (8) Å. The ratio of the integrated intensities of these two peaks at high– and low–r is of 0.008/0.140, that is about 5.7 per cent, a figure which becomes fairly close to the ratio of poled/unpoled material.

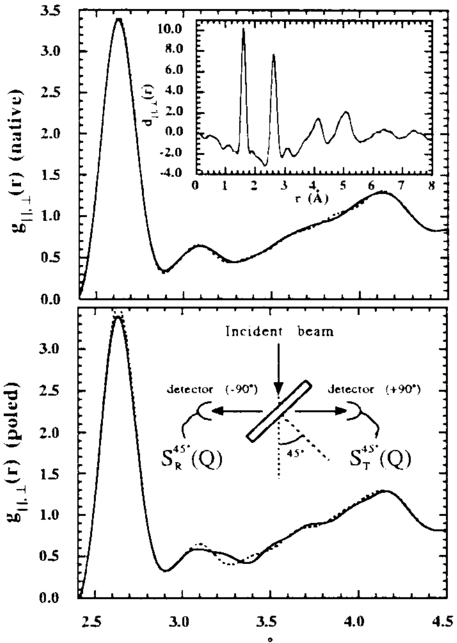

FIG. 1. A comparison between the radial distribution functions for native (upper frame) and poled (lower frame) samples. In both cases, the dashed lines depict the functions $g_{\|}(r)$ whereas the functions $g_{\perp}(r)$ are shown by solid lines. The inset in the upper frame displays the measured $d_{\|,\perp}(r)$ for the native sample comprising a wider range of distances. The inset in the lower frame shows the geometrical arrangement corresponding to the sample at 45° with respect to the incident beam. The spectra needed to calculate the distribution functions are obtained as $S_{\|,\perp}(Q) = (S^{45°}_{T,R}(Q) + S^{-45°}_{T,R}(Q))/2$ where T and R denotes transmitted and reflected and 45° and −45° the angle of the sample with respect to the incident beam as shown in the figure

Some additional alterations in the glass structure are revealed in the difference function $\Delta d(r) = d_{\mathrm{poled}}(r) - d_{\mathrm{unpoled}}(r)$ between poled and unpoled samples, this time $d(r)$ being evaluated from an average taken over all detectors. There, a negative peak appearing at 4.4 Å merits to be commented on, since this corresponds to a real-space manifestation of a difference in height of the first diffraction peak which shows its maximum at ≈ 1.5 Å^{-1}. The observed effects are commensurable with the increase in the Si–Si distance upon poling since Si–O, O–O and Si–Si correlations contribute to the first peak in $S(Q)$ with an in-phase oscillation in their partial structure factors, and therefore a mismatch of one of these correlations will lead to a decrease in the peak height.

The microscopic details of the structure within the poled region are difficult to access because of the weakness of the signals and the mechanism by which how this happens can only be a matter of educated guessing. However, both the value of 3.22 Å of the Si–Si distance within the poled zone as well as the decrease in correlations about 4 Å provide indications of a structure more open than that of the native glass which arises in the direction perpendicular to the plate surface as a consequence of poling. The value for the Si–O–Si bond angle would then reach some 167°, which although far larger than that of 142° of the unpoled glass sits within the range of values found for some polymorphs of SiO_2 (see Table I of [7]). On the other hand, most of the known structures of the disordered phases of SiO_2 show fairly wide distributions for the referred angle, meaning that values as large as that quoted above still have a very substantial probability of occurrence.

The possibility of inducing a transformation from the isotropic glass to a less disordered form can be understood on the basis of recent results [8], which show how disordered crystal phases can be formed from a glassy (or deeply supercooled) state. In the particular case of silica polymorphs a common parent structure corresponding to a disordered b.c.c. crystal can be found, from where the known forms of SiO_2 can be derived [9] by ordering and displacive mechanisms which involve pressure and the degree of occupancy of the b.c.c. structure by oxygen atoms. It seems then plausible to expect an ordering transition between the fully disordered and some partially ordered structure occurring via the referred cubic crystal as a consequence of the aligning electric-field. Large scale particle rearrangements within the glassy matrix can be expected to occur under the harsh conditions of poling (See for instance [10]).

The resulting structure may show some (albeit limited) analogy with those reported for low-density SiO_2 polymorphs. In this respect, it is worth recalling that the presence of regions with $\alpha-$ and $\beta-$cristobalite-like structures in v-SiO_2 was postulated time ago [11] as a means to explain the observed anomalies in the elastic properties as well as in the thermal expansion and specific heat. Also, the proximity of the short-range structures (5 – 10 Å) of vitreous silica and $\beta-$cristobalite have been demonstrated very recently by total diffraction measurements [12]. In our particular case, such points of contact are established on the grounds of: (a) a density which is close to that of the glass, so that a transformation at ambient pressure can be envisaged, (b) the need of performing the poling at temperatures not lower than those where $\beta-$cristobalite becomes the stable crystalline form of SiO_2, and finally (c) the rather open Si–O–Si bond angle indicative of great flexibility in the inter-tetrahedral angle. The parallelism cannot be drawn in full since all the details seen in Fig. 1 cannot be accommodated within the structure known for bulk $\beta-$cristobalite.

We are now starting molecular dynamics simulations for which the collected data constitutes an invaluable benchmark. Further more, a new battery of experiments are underway or planned: from a recently collected neutron reflectometry data we hope to gain information about the "active" layer in the material responsible of the SHG; a muon scattering experiment now underway, should gives us a quantitative assessment of any electrostatic field "frozen-in" inside the material; finally, we have planned a neutron diffraction experiment designed to explore not only anisotropy but breakdown of centrosymmetry.

---

[1] U. Osterberg and W. Margulis, Opt. Lett. **11**, 516 (1986).

[2] A. Yariv and P. Yeh, *Optical waves in crystals*, Wiley, 1984, p. 504.

[3] E.M. Dianov *et al.*, Sov. Lightwave Commun. **1**, 247 (1991); D.Z. Anderson, *et al.* Opt. Lett. **16**, 796 (1991).

[4] R. A. Myers *et al.*, Opt. Lett. *16*, 1732 (1991).

[5] C. Cabrillo *et al.*, Phys. Lett. **A248**, 257 (1998).

[6] C. Cabrillo *et al.*, Phys. Rev. Lett. **81**, 4361 (1998).

[7] P. Vashista *et al.*, Phys. Rev. **B41**, 12197 (1990).

[8] R. Fayos *et al.*, Phys. Rev. Lett. **77**, 3852 (1996).

[9] V. Dmitriev *et al.*, Europhys. Lett. **37**, 553(1997).

[10] M. Qiu *et al.*, J. Opt. Soc. Am. B **15**, 1362 (1998).

[11] M.R. Vukcevich, J. Non-Cryst. Solids **11**, 25 (1972).

[12] I.P. Swainson and M.T. Dove, J. Phys. C **7**, 1771 (1995); M.T. Dove *et al.*, Phys. Chem. Minerals, **24**, 311 (1997).